A Scalable Algorithm for the Optimal Trajectory of a Massive Swarm of UAV Base Stations Using Lagrangian Mechanics

Marceau Coupechoux*, Jérôme Darbon †, Jean-Marc Kélif‡, and Marc Sigelle§
*Telecom Paris, France, †Brown University, US, ‡Orange Labs, France, §On leave from Telecom Paris, France
Emails: marceau.coupechoux@telecom-paris.fr, jerome_darbon@brown.edu,
jeanmarc.kelif@orange.com, marc.sigelle@gmail.com

***Abstract*—In this paper, we consider multiple Unmanned Aerial Vehicles (UAV) serving as flying Base Stations (BS) of a wireless network and the problem of jointly optimizing their trajectory with respect to a running cost. This cost accounts for the consumed energy related to the vehicle velocity and for the amount of data traffic collected or served by the UAVs. The data traffic is supposed to be spatially distributed around a hotspot and is equivalent to a potential in Physics. Using the principles of Lagrangian Mechanics, we derive a scalable algorithm able to optimize the trajectory of thousands of drones in milliseconds on a off-the-shelf laptop. Our model allows to control the distance between the UAVs to avoid collisions by using a coupling between the drone trajectories.**

I. Introduction

Unmanned Aerial Vehicles (UAV) are expected to be part of future 6G networks. UAVs are indeed able to complement the traditional cellular networks by providing a very flexible way of enhancing coverage or capacity. UAVs can also serve as relays for distant users or collect information from Internet of Things (IoT) sensors. Several use cases show the interest of deploying multiple UAVs for efficiency, complementary, fault tolerance, or cost reasons [1]. In all these applications, a coordinated path-planning problem arises [2]. On the one hand, the UAVs should maximize the amount of data traffic to serve or the amount of information to collect. On the other hand, the energy consumed along the trajectory should be minimized. Coordinating multiple UAVs is usually facing additional issues like collision avoidance. An important limitation is related to scalability: designing optimal trajectories is usually feasible only for very few UAVs due to the complexity of the problems at hand. In this paper, we thus propose a new approach, based on Hamilton-Jacobi-Bellman (HJB) equations and Lagrangian Mechanics, that is able to solve the multi-UAV trajectory problem for thousands of UAVs at a click speed.

II. Related Works

The problem of optimizing the trajectory of multiple *communicating* UAVs has been recently tackled in the literature for various use cases and using various analytical approaches. A classical solution stems from earlier single-UAV trajectory optimization studies, see e.g. [3]. It consists in discretizing time or space and formulating a mixed integer non-convex optimization problem [4]. Sub-optimal solutions are usually achieved thanks to combinations of block descent and Successive Convex Approximation (SCA) algorithms. For example, in [5], multiple-UAV are serving ground users in the downlink. Association, scheduling, UAV trajectory and power control are optimized to maximize the minimum throughput to ground users. This leads to a mixed integer non-convex problem that is solved using block coordinate descent and successive convex optimization. Numerical results involve only two UAVs. In [6], authors consider a system in which every UAV communicates with a dedicated ground station. Authors formulate a joint trajectory and power control problem for maximizing the aggregate sum rate with a constraint for collision avoidance. The solution is based on SCA. A parallel algorithm is proposed to gain in computation time. Up to 20 UAVs are considered in the simulations. Authors of [7] propose a model in which UAVs serve as mobile edge computing servers for IoT users. The considered problem is non-convex and is thus decomposed into subproblems, including the trajectory optimization. Numerical experiments involve 4 UAVs. In [8], a scenario is described in which UAVs transfer energy to ground IoT devices, which in turn upload their data. A non-convex optimization problem is derived and solved using an alternative iteration algorithm. Two UAVs are considered. In [9], authors provide a mixed integer formulation of the trajectory problem involving routing, scheduling and communications constraints for UAV fleets. Numerical experiments do not consider more than six UAVs. The reference [10] proposes a system in which multiple UAV are tracking ground mobile vehicles. A joint optimization problem involving the trajectory of the UAVs and constraints for collision avoidance is formulated. Time is slotted and the problem is solved using SCA. Only two UAVs are considered in the numerical results. We see that this approach can be taylored to various scenarios and is able to take into account various constraints related to the UAV and the communication models. However, it fails to scale beyond few UAVs. A recent set of papers has tackled the problem using Reinforcement Learning (RL), see the Related Work section of [11]. The problem is generally formulated by using a Markov Decision Process (MDP) or a MDP variant or a game depending on the amount of available information and the number of agents. Actions are generally related to the direction, speed or acceleration of the UAVs.

The reward is related to the communication objectives and energy constraints. For example, [12] considers a system in which UAVs offload tasks for ground users. The goal is to minimize the energy consumption by optimizing the offloading decisions and the UAV trajectories. The solution is based on a multi-agent reinforcement learning algorithm. Up to 4 UAVs are considered in numerical results. Authors of [13] propose a model in which multiple UAVs are tracking multiple first responders thanks to noisy distance measurements. The problem is formulated by a MDP and solved using Deep RL. Up to eight UAVs are considered in the experiments. In [14], a scenario is proposed in which multiple UAV deliver content to ground stations. Authors aim at maximizing the energy efficiency under various constraints. To take into account the environment uncertainties, the problem is modeled with two coupled stochastic games. Decentralized learning algorithms are proposed to solve it. Three UAVs are considered in the numerical results. These approaches have the advantage of being decentralized as they can be deployed in every UAV, but again they fail to tackle the scalability issue. They are also adapted to specific scenarios: if the scenario conditions are changing, the learning process, which is a time-consuming part of these solutions, has to be relaunched. In a previous work [15], we have proposed a completely new approach, which is both generic and much less complex than existing solutions. The approach is based on principles of the Lagrangian Mechanics (the UAV is seen as a particle subjected to a kinetic and potential energy) and relies on the solutions of the HJB equations. Closed-form expressions of the trajectory have been obtained for a single UAV for different forms of the potential. In this paper, we extend the approach to multiple-UAV and show how we can overcome the curse of dimensionality. The only reference in the literature employing similar tools is [16]. Authors propose a scenario in which UAVs are deployed to transmit cached content to a ground users. A stochastic differential game is formulated to optimize the quality of experience of the users. A limiting problem is considered and a mean-field approach is considered. A HJB Fokker-Planck-Kolmogorov (FPK) equation is derived to find the mean-field equilibrium. A DNN based algorithm is proposed to reduce the solution complexity. This approach allows authors to consider up to 30 UAVs in their numerical experiments. We develop here an analysis for thousands of UAVs.

Other numerical approaches rely on numerically solving the Hamilton-Jacobi Partial Differential Equation associated with the optimal control problem. Several recent methods have been proposed to solve HJ Partial Differential Equations (PDE) in high dimensions, see e.g., [17], [18]. However, to our knowledge, these approaches above do not apply to the models considered in this paper: specifically, these approaches cannot cope with Hamiltonians corresponding to harmonic oscillators.

III. Recalls on the Single-UAV Trajectory Model

In this short section, we start by recalling our results for a single UAV [15] and we introduce the notations of the paper. We intend to control the trajectory and the velocity of a single UAV Base Station (BS) evolving in a physical Euclidian space $E = \mathbb{R}^d$ ($d = 2$ or 3). $\mathbb{R}^d$ is endowed with the natural norm $\|z\|^2$ and scalar product $x \cdot y$. The drone evolves during the time interval $\mathcal{I} = [t_0, T]$ between respective locations $z^0 \triangleq z(t_0)$ at $t = t_0$ and $z^T \triangleq z(T)$ at $t = T$ around a traffic *hotspot/hole* while minimizing a *total cost* determined by all velocities and instantaneous traffics see (9). The (time-stationary) traffic model has the following form:

$$u(z) = u(t, z) = \frac{1}{2} u_0 \|z - z_h\|^2 \tag{1}$$

where z_h is the traffic node. The UAV BS is able to cover an area, from which it can serve users. Its velocity noted $a = \dot{z} = dz/dt$, induces an energy cost. The *running cost* (Lagrangian) is

$$\mathcal{L}(z, a) = \frac{K}{2}\|a\|^2 - \frac{1}{2} u_0 \|z - z_h\|^2 \tag{2}$$

where the first term (kinetic part) $E_c(a) = \frac{K}{2}\|a\|^2$ is related to the vehicle velocity. The higher is the speed, the higher is the energy cost. The second term (potential part) $u(z)$ is the *user traffic intensity* served by the UAV BS.

To *minimize* the total cost (action) $\int_{t_0}^{T} \mathcal{L}(z, a)\, dt$ a trajectory has to satisfy the variational Euler-Lagrange equation

$$\frac{d}{dt} \nabla_a \mathcal{L}(z^*(t), a^*(t)) = \nabla_z \mathcal{L}(z^*(t), a^*(t)) \tag{3}$$

$$\Rightarrow \ddot{\bar{z}}^* + \alpha\, \omega^2\, \bar{z}^* = 0 \tag{4}$$

where $\bar{z}^* = z^* - z_h$ is the *centered* instantaneous position vector on z_h and where $u_0 = \alpha\, K\omega^2$ ($\alpha = \pm 1$). This yields the following types of optimal trajectory [19], [20].

- For $u_0 = -K\omega^2 < 0$ (*hotspot*, "hyperbolic case"):

$$\bar{z}^*(t) = \frac{\bar{z}^T \sinh(\omega(t - t_0)) + \bar{z}^0 \sinh(\omega(T - t))}{\sinh(\omega(T - t_0))} \tag{5}$$

where $\bar{z}^0 = z^0 - z_h$ and $\bar{z}^T = z^T - z_h$.

- For $u_0 = +K\omega^2 > 0$ (traffic *hole*, "elliptic case" - the well-known "harmonic oscillator" model of Physics):

$$\bar{z}^*(t) = \frac{\bar{z}^T \sin(\omega(t - t_0)) + \bar{z}^0 \sin(\omega(T - t))}{\sin(\omega(T - t_0))} \tag{6}$$

- The third case $u_0 = 0$ corresponds to a free particle with uniform linear movement and will also appear later.

It will be convenient to employ the following notation:

$$\text{Let define } u^\alpha_\omega(\tau) = \begin{cases} \sinh \omega\, \tau \,/\, \omega & \alpha = +1 \\ \sin \omega\, \tau \,/\, \omega & \alpha = -1 \\ \tau & \alpha = 0\ (\omega = 0) \end{cases}$$

$$\text{and} \quad \phi^\alpha_\omega(t) = \frac{u^\alpha_\omega(T - t)}{u^\alpha_\omega(T - t_0)} \quad , \quad \psi^\alpha_\omega(t) = \frac{u^\alpha_\omega(t - t_0)}{u^\alpha_\omega(T - t_0)} \tag{7}$$

These two functions are independent [1] and designed so that

$$\phi^\alpha_\omega(t_0) = 1 \ , \phi^\alpha_\omega(T) = 0$$
$$\psi^\alpha_\omega(t_0) = 0 \ , \psi^\alpha_\omega(T) = 1$$
$$\Rightarrow \bar{z}(t) = \bar{z}_0\, \phi^\alpha_\omega(t) + \bar{z}^T\, \psi^\alpha_\omega(t) \tag{8}$$

[1] apart when $\alpha = -1$, $\omega\,(T - t_0) = n\pi$, $n \in \mathbb{N}^*$ which we discard here.

Coupling UAV's will lead to combine two among these three trajectory models ('mixing' of modes) as will be shown later.

IV. Multi-UAVs with Single Hotspot Model

In this paper we tackle the multi-UAV, single hotspot trajectory problem first for uncoupled then for coupled UAVs.

A. Uncoupled and Independent UAVs

In this part N drones having the same (positive) mass K evolve independently around the *same* traffic *hotspot / hole* z_h during the *same* time interval $\mathcal{I} = [t_0, T]$ and all with the same traffic model (1). as before. Their locations are $z_k^0 \triangleq z_k(t_0)$ at time $t = t_0$ and $z_k^T \triangleq z_k(T)$ at time $t = T$ with $k = 1, \ldots, N$. Their velocities are $a_i = \dot{z}_i = dz_i/dt$. The running cost of the system is clearly the sum of all the running costs of the independent drones:

$$\mathcal{L}(t, Z, A) = \sum_{i=1}^{N} \left(\frac{K}{2} \|a_i\|^2 - \frac{1}{2} u_0 \|z_i - z_h\|^2 \right) \quad (9)$$

This enables to define the 'total configuration' vector space

$$F = E^N = (\mathbb{R}^d)^N = \mathbb{R}^{N \times d}$$

and the respective total 'position' and 'velocity' vectors

$$Z = (z_1, z_2 \ldots z_N) \text{ and } A = (a_1, a_2 \ldots a_N) = \dot{Z} \in F$$

F is naturally endowed with the induced Euclidean norm

$$|||Z|||^2 = \sum_{i=1}^{N} \|z_i\|^2 \quad \forall Z = (z_1, z_2 \ldots z_N) \in F \quad (10)$$

and related scalar product $\langle X, Y \rangle = \sum_{i=1}^{N} x_i \cdot y_i, \forall X, Y \in F$.
Noting the total 'hotspot configuration' as

$$Z_h = (z_h, z_h \ldots z_h)$$

then the running cost writes in this formalism as

$$\mathcal{L}(Z, A) = \frac{K}{2} ||| A |||^2 - \frac{u_0}{2} ||| Z - Z_h |||^2$$

In the sequel we assume a *hotspot* traffic model (i.e., $\alpha = 1$) so that the associated running cost (2) is

$$\mathcal{L}(Z, A) = \frac{K}{2} [|||A|||^2 + \omega^2 ||| Z - Z_h |||^2].$$

B. Coupled Multi-UAVs

Consider now the quadratic form (on F)

$$\phi(Z) = \sum_{\substack{i<j \\ i,j=1:N}} \|z_i - z_j\|^2$$

In this work we include the drone *coupling* potential

$$U(Z) = v_0 \ \phi(Z)$$

as a third term in the total running cost, with the goal to (also) control the distances between the UAVs. We then diagonalize this resulting total running cost in order to decompose optimal trajectories as sums of proper 'modes' of the form (7)(8) For this, we define the linear *replica* mapping χ ('copy') as

$$\begin{array}{lll} E = \mathbb{R}^d & \mapsto & F = \mathbb{R}^{N \times d} \\ T \in E & \mapsto & \chi(T) = \underbrace{(T, T \ldots T)}_{N \text{ times}} \end{array}$$

Note that the single hotspot hypothesis writes in this frame as

$$Z_h = \chi(z_h)$$

Now the main property of quadratic form $\phi(Z)$ is that it is *invariant* by *any same* translation of all (UAVs) positions i.e.,

$$\phi(Z) = \phi(Z + \chi(T)) \quad \forall T \in E \quad (\text{cf. } \textit{Laplacian})$$

Thus it is null when all z_i are *equal* (take $T = -z_i \, \forall i = 1 : N$). This latter result allows easy diagonalization of ϕ since [2]

$$\begin{aligned} \phi(Z) &= (N-1) \sum_{i=1}^{N} \|z_i\|^2 - 2 \sum_{i<j} z_i \cdot z_j \\ &= N \sum_{i=1}^{N} \|z_i\|^2 - \left[\sum_{i=1}^{N} \|z_i\|^2 + 2 \sum_{i<j} z_i \cdot z_j \right] \\ &= N \sum_{i=1}^{N} \|z_i\|^2 - \| \sum_{i=1}^{N} z_i \|^2 \qquad (11a) \\ &= N \left(\sum_{i=1}^{N} \|z_i - \frac{1}{N} \sum_{i=1}^{N} z_i\|^2 \right) \qquad (11b) \end{aligned}$$

Now let define the linear *barycenter* mapping M ('mean') as

$$\begin{array}{lll} F = \mathbb{R}^{N \times d} & \mapsto & E = \mathbb{R}^d \\ Z = (z_1, z_2 \ldots z_N) \in F & \mapsto & MZ = g = \frac{1}{N} \sum_{i=1}^{N} z_i \end{array}$$

Then (11b) is written as

$$\phi(Z) = N \ ||| Z - \chi(g) |||^2 \text{ with } g \text{ barycenter of } \{z_i\} \quad (12)$$

At this point

- It is already known that any 'copy vector' $\chi(T) = (T, T \ldots T) \in F$ annuls ϕ. Thus the linear subspace $H = \text{Im}(\chi)$ is an eigenspace of the quadratic form ϕ associated to eigenvalue 0.
- Now the (linear) orthogonal subspace of H in F, is the set $H^\perp$ of vectors $Z \in F$ such that

$$\langle Z, \chi(T) \rangle = \sum_{i=1}^{N} z_i \cdot T = 0 \quad \forall T \in E \Leftrightarrow \sum_{i=1}^{N} z_i = 0 \ !$$

The *orthogonal* decomposition of a vector $Z \in F$ onto both subspaces H and $H^\perp$, noted

$$Z = \underbrace{A}_{\in H^\perp} \oplus \underbrace{B}_{\in H} \quad (13)$$

is simply $Z = (Z - \chi(x)) \oplus \chi(x)$ for some $x \in E$.
To find the adequate vector x we note that $Z - \chi(x) \in H^\perp$

$$\begin{aligned} \Rightarrow \sum_{i=1}^{N} (z_i - \chi(x)_i) = \sum_{i=1}^{N} (z_i - x) &= 0 \\ \Rightarrow x = g = \frac{1}{N} \sum_{i=1}^{N} z_i &= MZ \end{aligned}$$

[2] (11a) is the intra-variance equivalence and (11b) is the Huyghens theorem.

Thus the decomposition

$$Z = (Z - \chi\,(g)) \oplus \chi\,(g) \text{ with } g = MZ, \text{ is orthogonal in } F.$$

Since $H^\perp$ is precisely the space of vectors $Y \in F$ such that $MY = 0$, it follows readily from (12) that

$$\phi(Y) = N \,|||\, Y \,|||^2 \quad \forall Y \in H^\perp \;\; !$$

To summarize, quadratic form ϕ has two eigenvalues:

- $\lambda = 0 \to$ eigenspace H
- $\lambda = N \to$ eigenspace $H^\perp$

Now in order to diagonalize the total quadratic running cost (and at each time) we use the following property:

$$\forall t \in [t_1, t_2)\; X(t) \in V \text{ linear subspace of } F \Rightarrow \dot{X}(t) \in V$$

(right derivative) and idem for left derivative in $(t_1, t_2]$.
Proof is straightforward since calculus yields indeed:

$$\frac{X(t+h) - X(t)}{h} \in V \;\forall h > 0,\; t,\; t+h \in [t_1, t_2) \square$$

Now, since V is complete as a finite dimension vector space:

$$\Rightarrow \dot{X}(t) = \lim_{h \to 0^+} \frac{X(t+h) - X(t)}{h} \in V$$

It follows that if vector $\bar{Z}(t)$ has the orthogonal decomposition $\bar{Z}(t) = \underbrace{\xi(t)}_{\in H^\perp} \oplus \underbrace{\gamma(t)}_{\in H}$ $\forall t \in \mathcal{I}$ then also for time derivatives: $\dot{\bar{Z}}(t) = \dot{\xi}(t) \oplus \dot{\gamma}(t)$ and the norm property holds (Pythagoras)

$$\begin{aligned} |||\bar{Z}(t)|||^2 &= |||\xi(t)\,|||^2 + |||\,\gamma(t)|||^2 && \forall t \in \mathcal{I} \\ |||\dot{\bar{Z}}(t)|||^2 &= |||\dot{\xi}(t)\,|||^2 + |||\,\dot{\gamma}(t)|||^2 && \forall t \in \mathcal{I} \end{aligned}$$

We apply these results to the centered position variable around hotspot z_h:

$$\bar{Z} = Z - \chi\,(z_h),$$

a variable which enjoys the straightforward properties:

- $\Phi(\bar{Z}) = \phi(Z)$ by translation invariance.
- $\dot{\bar{Z}} = \dot{Z} = A$ (velocities).

Similarly we shall define and use the centered variable

$$\bar{g} = g - z_h$$

All related definitions and properties are shown in Table I

first noting $g \;= MZ \;,\;\; \bar{g} = M\bar{Z}$	$= g - z_h \quad \Rightarrow$	
then $\gamma = \chi\,(M\bar{Z}) = \chi\,(\bar{g})$	$= \chi\,(g - z_h) \in H$	
$\xi = \bar{Z} - \gamma = \bar{Z} - \chi\,(\bar{g})$	$= Z - \chi\,(g) \in H^\perp$	

TABLE I: Single hotspot coupled model: properties.

The decomposition of total running cost $\bar{\mathcal{L}}(\bar{Z}, A)$ is shown in Table II Eqs. (14a)-(14b). The coupling interaction constant is defined as $v_0 = -\epsilon\; K\Omega^2/2$ with $\epsilon = \pm 1$ (*hyperbolic / elliptic*.) It was shown in [15] that for a *hotspot* model (i.e., concave quadratic traffic) increasing the quadratic parameter ω^2 leads to trajectories closer to the hotspot. Similarly here coupling interaction with $\epsilon = +1$ attracts drones trajectories together.
This leads in turn to separate Euler-Lagrange equations since

$$\begin{aligned} \nabla_{\bar{Z}}\, \bar{\mathcal{L}} &= \nabla_\xi\, \bar{\mathcal{L}} \oplus \nabla_\gamma\, \bar{\mathcal{L}} \\ &= K\,(\,(\omega^2 + \epsilon\, N\, \Omega^2)\, \xi \oplus \omega^2\, \gamma\,) \\ \nabla_A\, \bar{\mathcal{L}} &= \nabla_{\dot{\xi}}\, \bar{\mathcal{L}} \oplus \nabla_{\dot{\gamma}}\, \bar{\mathcal{L}} \\ &= K\,(\,\dot{\xi} \oplus \dot{\gamma}\,) \\ \to \frac{d}{dt} \nabla_A\, \bar{\mathcal{L}} &= K\,(\,\ddot{\xi} \oplus \ddot{\gamma}\,) \end{aligned}$$

therefore the Euler-Lagrange equation *wrt.* variable $\bar{Z}$ reads

$$\frac{d}{dt} \nabla_A\, \bar{\mathcal{L}} - \nabla_{\bar{Z}}\, \bar{\mathcal{L}} = K\big(\,(\ddot{\xi} - (\omega^2 + \epsilon N \Omega^2)\,\xi) \oplus (\ddot{\gamma} - \omega^2\,\gamma)\,\big).$$

This quantity should be the null vector of $F = \mathbb{R}^{N \times d}$ so one readily obtains the separate Euler-Lagrange equations

$$\ddot{\xi} - \,(\omega^2 + \epsilon\, N\, \Omega^2)\, \xi = 0 \text{ and } \ddot{\gamma} - \;\omega^2\, \gamma = 0$$

• Now recall that $\gamma(t) = \chi\,(\bar{g}(t))\;\; \forall t \in \mathcal{I}$ (and thus $|||\gamma(t)|||^2 = N \|\bar{g}(t)\|^2$) so that the (centered!) barycenter of the N drones $\bar{g}(t) = g(t) - z_h$, follows a *single* drone *hyperbol* arc with *effective* mass $N \times K$ and *fundamental* pulsation ω ("mode") *whatever* the coupling constant value v_0, between its original and final positions $\gamma(t_0)$ and $\gamma(T)$.
• The projection of $\xi(t)$ on the canonical subspace E_i associated to drone $\#i \in 1, \ldots, N$ namely: $\xi_i = z_i(t) - g(t)$, follows an effective trajectory with mass K between its original and final values. From (4) all these trajectories have the same type and effective pulsation given by the parameters $\eta \in [-1, 0, +1]$ and $\bar{\Omega} \geq 0$ appearing in the following formula

$$\eta\; \bar{\Omega}^2 = \omega^2 + \epsilon\;\, N\;\, \Omega^2 \quad i.e., \tag{15}$$

a) for $\eta = +1$ (e.g. when $\epsilon > 0$) an *hyperbol* arc (5) with effective pulsation $\bar{\Omega}$,
b) for $\eta = -1$ (happens in case $\epsilon = -1$ only) an *ellipse* arc (6) with effective pulsation $\bar{\Omega}$ (harmonic oscillator),
c) for $\bar{\Omega} = 0$ (happens in case $\epsilon = -1$ only, and $\eta = 0$ by convention) a uniform *linear* movement (free drone).

The related "cut-off" pulsation of case c) which also separates regimes a) and b), is given by $\Omega = \Omega_0 = \dfrac{\omega}{\sqrt{N}}$.

To summarize, using notations (7) and (8) together with

$$Z^0 = (z_k^0) \;\;, Z^T = (z_k^T) \;\;,\;\; g^0 = MZ^0 \;\;,\;\; g^T = MZ^T \tag{16}$$

one has

$$\begin{aligned} \gamma_k(t) \quad &= g(t) - z_h && \forall k = 1, \ldots, N \\ &= (g^0 \;\, - z_h)\, \phi_\omega^{+1}(t) && + (g^T - z_h)\, \psi_\omega^{+1}(t) \\ \xi(t) \quad &= Z(t) - \chi\,(g(t)) && \\ &= (Z^0 - \chi\,(g^0))\, \phi_{\bar{\Omega}}^\eta(t) && + (Z^T - \chi\,(g^T))\, \psi_{\bar{\Omega}}^\eta(t) \\ \Rightarrow Z(t) \quad &= \chi\,(z_h) + \bar{Z}(t) && \\ &= \chi\,(z_h) + \xi(t) + \gamma(t) && \end{aligned}$$

$$\bar{\mathcal{L}} = \frac{K}{2}\ [\ \|\dot{\bar{Z}}\|^2 \qquad +\omega^2\ \|\|\ \bar{Z}\|\|^2\ +\ \epsilon\ \Omega^2\ \phi(\bar{Z})\ ] \tag{14a}$$

$$= \frac{K}{2}\ [\ \|\|\ \dot{\xi}\ \|\|^2 + \|\|\ \dot{\gamma}\|\|^2 \qquad +\omega^2\ (\ \|\|\xi\ \|\|^2 + \|\|\ \gamma\|\|^2\ ) + \ \epsilon\ \Omega^2\ (\ N\times \|\|\xi\ \|\|^2 + 0\times\|\|\gamma\|\|^2\ )\ ]$$

$$= \frac{K}{2}\ [\ \|\|\ \dot{\xi}\ \|\|^2 + \ (\omega^2 + \epsilon\, N\, \Omega^2)\ \ \|\|\ \xi\ \|\|^2\ ] \qquad + \frac{K}{2}\ [\ \|\|\ \dot{\gamma}\ \|\|^2 + \omega^2\ \ \|\|\ \gamma\ \|\|^2\ ] \tag{14b}$$

TABLE II: The total running cost for single hotspot and coupled multi-UAVs. Here $Z_h = \chi\,(z_h)$ and $\bar{Z} = Z - Z_h = \xi \oplus \gamma$

Finally the trajectory of each drone $\#k$ can be written as

$$z_k(t) = z_h + \underbrace{(z_k - g)}_{\xi_k}(t) + \underbrace{(g - z_h)}_{\gamma=\gamma_k} \qquad \forall k = 1, \ldots, N$$

i.e., the sum of two 'modes' trajectories plus a constant drift. We thus obtain an exact formulation of the trajectories that can be computed in linear time as a function of the number of UAVs.

V. Numerical Experiments

The experimental settings are shown in Table III.

⋆ Time interval is always chosen as $\mathcal{I} = [t_0, T] = [0, 2]$.
⋆ It is discretized in 50 elements, yielding discrete interval noted as $\mathcal{I}_d$.
⋆ Traffic constant $\omega = 1$ is the same for each hotspot and each example.
⋆ Here Ω is chosen proportional to Ω_0 with some selected coefficients.

TABLE III: common features to all experiments

We present results for $N = 20$ UAV's: without loss of generality, starting positions (A_n) are located on a circular arc and final ones (B_n) on a cubic spline. The hotspot is located near the center of gravity of all these points namely $z_h = [12; 10]$. Also for this set of parameters one obtains:
$N = 20,\ K = 1,\ \omega = 1 \rightarrow\ \Omega_0 = \dfrac{\omega}{\sqrt{N}} = 0.2236.$
This low value due to high N implies small behaviour changes in trajectories for similar values of Ω (especially for the attractive coupling) see Fig. 1. In order to check possible collisions we assign the drone with label 15 (initial position A_{15}) to final position $[19; 12]$ so that its trajectory crosses those of labels $\in [16..19]$. Computation of minimal distances in time shows that there is no time index at which collision occurs (i.e., the minimal distance is always strictly positive). For the scalability study, we use Scilab 2023.0.0 running on an AMD Ryzen 5 5600H processor. The algorithm has then linear CPU complexity *wrt.* N as seen in Figure 2. The optimal trajectory of 10 000 UAVs is obtained in 20 ms.

VI. Conclusion

In this work, we have considered the problem of optimizing the trajectory of a swarm of UAV Base Stations in a wireless network. The problem consists in minimizing a running cost along the trajectories of the UAVs, where the cost is made of an energy cost related to velocity and a negative part representing the amount of data traffic collected or served by the base stations. The traffic is spatially distributed around a hotspot. The analogy with the Lagrangian mechanics allows us to derive a simple algorithm that jointly optimizes the UAV trajectories. We have introduced a coupling between the trajectories to avoid drone collisions. Numerical experiments show that we obtain results for thousands of UAVs at a click speed. Future works include the definitions of more realistic traffic models, e.g. with multiple hotspots.

References

[1] G. Skorobogatov, C. Barrado, and E. Salamí, "Multiple UAV Systems: A Survey," *Unmanned Systems*, vol. 8, no. 2, pp. 149–169, apr 2020. [Online]. Available: www.worldscientific.com

[2] Y. Zhou, B. Rao, and W. Wang, "UAV Swarm Intelligence: Recent Advances and Future Trends," *IEEE Access*, vol. 8, pp. 183 856–183 878, 2020.

[3] A. Meng, X. Gao, Y. Zhao, and Z. Yang, "Three-Dimensional Trajectory Optimization for Energy-Constrained UAV-Enabled IoT System in Probabilistic LoS Channel," *IEEE Internet of Things Journal*, vol. 9, pp. 1109–1121, 1 2022.

[4] Y. Zeng, Q. Wu, and R. Zhang, "Accessing from the Sky: A Tutorial on UAV Communications for 5G and beyond," *Proceedings of the IEEE*, vol. 107, no. 12, pp. 2327–2375, dec 2019.

[5] Q. Wu, Y. Zeng, and R. Zhang, "Joint Trajectory and Communication Design for Multi-UAV Enabled Wireless Networks," *IEEE Transactions on Wireless Communications*, vol. 17, no. 3, pp. 2109–2121, mar 2018.

[6] C. Shen, T. H. Chang, J. Gong, Y. Zeng, and R. Zhang, "Multi-UAV Interference Coordination via Joint Trajectory and Power Control," *IEEE Transactions on Signal Processing*, vol. 68, pp. 843–858, 2020.

[7] X. Qin, Z. Song, Y. Hao, and X. Sun, "Joint Resource Allocation and Trajectory Optimization for Multi-UAV-Assisted Multi-Access Mobile Edge Computing," *IEEE Wireless Communications Letters*, 2021.

[8] J. Wang, Z. Na, and X. Liu, "Collaborative Design of Multi-UAV Trajectory and Resource Scheduling for 6G-Enabled Internet of Things," *IEEE Internet of Things Journal*, vol. 8, pp. 15 096–15 106, 10 2021.

[9] N. R. Zema, E. Natalizio, L. D. P. Pugliese, and F. Guerriero, "3D Trajectory Optimization for Multimission UAVs in Smart City Scenarios," *IEEE Transactions on Mobile Computing*, pp. 1–11, 2022. [Online]. Available: https://ieeexplore.ieee.org/document/9925115/

[10] X. Liu, B. Lai, B. Lin, and V. C. Leung, "Joint Communication and Trajectory Optimization for Multi-UAV Enabled Mobile Internet of Vehicles," *IEEE Transactions on Intelligent Transportation Systems*, vol. 23, pp. 15 354–15 366, 9 2022.

[11] H. Bayerlein, M. Theile, M. Caccamo, and D. Gesbert, "Multi-UAV Path Planning for Wireless Data Harvesting With Deep Reinforcement Learning," *IEEE Open Journal of the Communications Society*, vol. 2, pp. 1171–1187, 2021. [Online]. Available: https://ieeexplore.ieee.org/document/9437338/

[12] L. Wang, K. Wang, C. Pan, W. Xu, N. Aslam, and L. Hanzo, "Multi-Agent Deep Reinforcement Learning-Based Trajectory Planning for Multi-UAV Assisted Mobile Edge Computing," *IEEE Transactions on Cognitive Communications and Networking*, vol. 7, pp. 73–84, 3 2021. [Online]. Available: https://ieeexplore.ieee.org/document/9209079/

[13] J. Moon, S. Papaioannou, C. Laoudias, P. Kolios, and S. Kim, "Deep Reinforcement Learning Multi-UAV Trajectory Control for Target Tracking," *IEEE Internet of Things Journal*, vol. 8, pp. 15 441–15 455, 10 2021.

[14] C. Zhao, J. Liu, M. Sheng, W. Teng, Y. Zheng, and J. Li, "Multi-UAV Trajectory Planning for Energy-Efficient Content Coverage: A Decentralized Learning-Based Approach," *IEEE Journal on Selected Areas in Communications*, vol. 39, pp. 3193–3207, 10 2021.

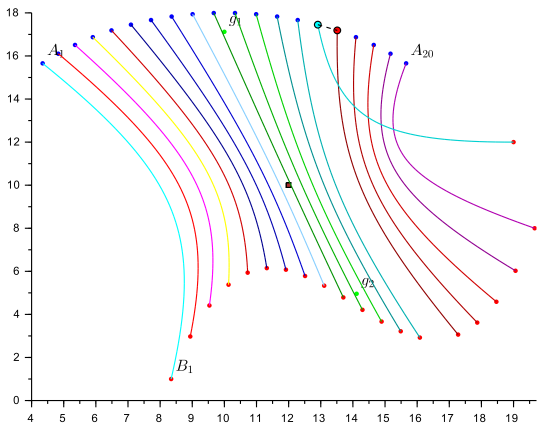

(a) $\Omega = 0$ no coupling - initial drone positions in blue

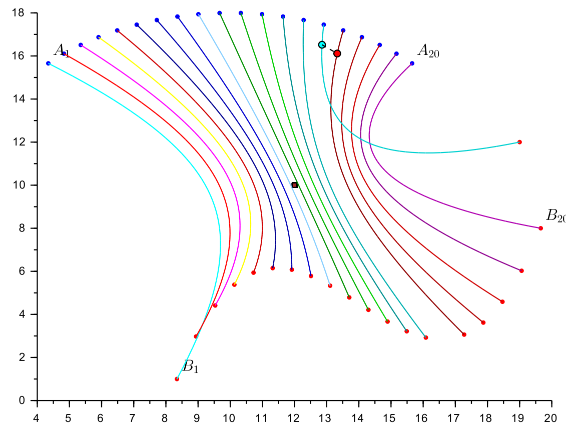

(b) attractive $\Omega = \Omega_0$ $(\eta = +1)$ - z_h appears in brown

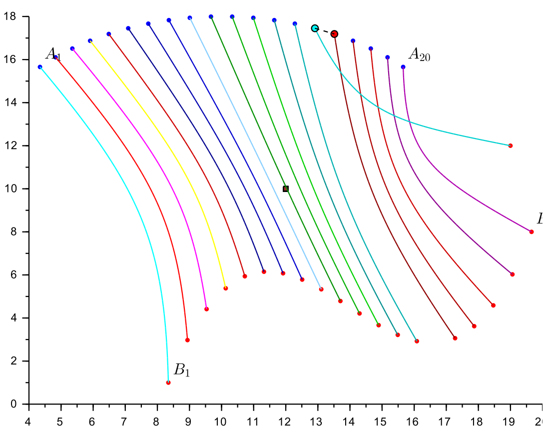

(c) repulsive $\Omega = 0.7\ \Omega_0$ $(\eta = -1)$

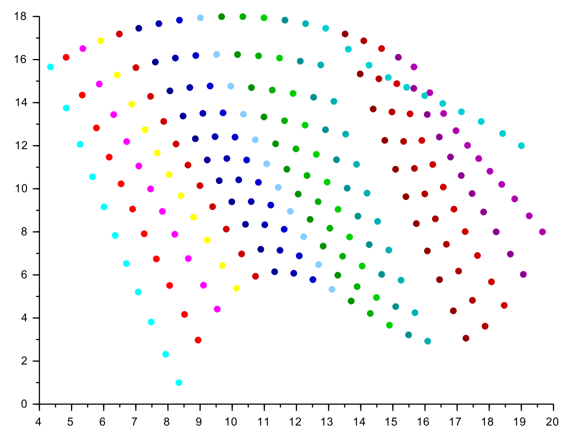

(d) trajectories of case repulsive ($\Omega = \Omega_0$, $\eta = -1$) sampled at time indices $\tau = [1{:}5{:}50,\ 50]$

Fig. 1: Single-hotspot model for $N = 20$. Snap of UAV #15 (light cyan) with its overall closest UAV is shown.

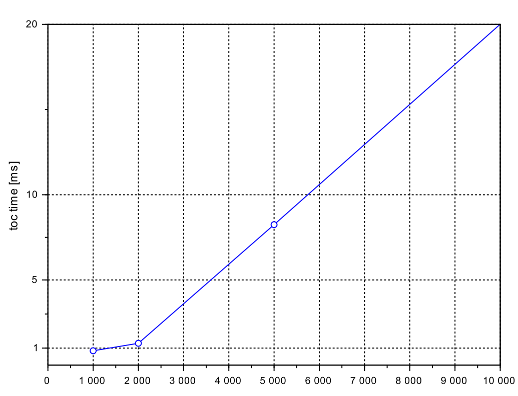

Fig. 2: Scalability: algorithm computing time vs. number of UAVs.

[15] M. Coupechoux, J. Darbon, J.-M. Kélif, and M. Sigelle, "Optimal Trajectories of a UAV Base Station Using Hamilton-Jacobi Equations," *arXiv preprint arXiv: Optimization and Control*, 2021. [Online]. Available: https://arxiv.org/abs/2102.02632

[16] S. Chai and V. K. Lau, "Multi-UAV Trajectory and Power Optimization for Cached UAV Wireless Networks with Energy and Content Recharging-Demand Driven Deep Learning Approach," *IEEE Journal on Selected Areas in Communications*, vol. 39, pp. 3208–3224, 10 2021.

[17] M. Akian, R. Bapat, and S. Gaubert, "Max-plus algebra," *Handbook of linear algebra*, vol. 39, 2006.

[18] J. Darbon and S. Osher, "Algorithms for Overcoming the Curse of Dimensionality for Certain Hamilton-Jacobi Equations Arising in Control Theory and Elsewhere," *Res Math Sci Research in the Mathematical Sciences*, vol. 3, no. 19, pp. 1–26, 2016. [Online]. Available: https://doi.org/10.1186/s40687-016-0068-7

[19] M. Coupechoux, J. Darbon, J.-M. Kelif, and M. Sigelle, "Optimal Trajectories of a UAV Base Station Using Lagrangian Mechanics," in *IEEE INFOCOM 2019-IEEE Conference on Computer Communications Workshops (INFOCOM WKSHPS)*. IEEE, 2019, pp. 626–631.

[20] ——, "Optimal Trajectories of a UAV Base Station Using Hamilton-Jacobi Equations," *IEEE Transactions on Mobile Computing*, vol. 22, no. 8, pp. 4837–4849, 2023.